MOL # 115303

1 # A small-molecule compound selectively activates K2P channel TASK-3 by

2 # acting at two distant clusters of residues

3 Fuyun Tian[1,2], Yunguang Qiu[1,2], Xi Lan[1,2], Min Li[3], Huaiyu Yang[4] and Zhaobing Gao[1,2]*

4 *[1]CAS Key Laboratory of Receptor Research, State Key Laboratory of Drug Research,*

5 *Shanghai Institute of Materia Medica, Chinese Academy of Sciences, Shanghai, 201203,*

6 *China. [2]University of Chinese Academy of Sciences, 19A Yuquan Road, Beijing, 100049,*

7 *China. [3] Department of Neuroscience, High Throughput Biology Center and Johns Hopkins*

8 *Ion Channel Center, School of Medicine, Johns Hopkins University, 733 North Broadway,*

9 *Baltimore, MD 21205. [4]Shanghai Key Laboratory of Regulatory Biology, Institute of*

10 *Biomedical Sciences, School of Life Sciences, East China Normal University, Shanghai,*

11 *200241, China*

12

13

14

15

16

17 **Running title:** NPBA is a selective TASK-3 channel activator

18 **Corresponding Author:**

19 Zhaobing Gao, CAS Key Laboratory of Receptor Research, State Key Laboratory of Drug
20 Research, Shanghai Institute of Materia Medica, Chinese Academy of Sciences, Shanghai,
21 201203, China.

22 Email: zbgao@simm.ac.cn

23 Phone: 86-21-2023 9067

24 **Document statistics:**

25 Text pages: 30

26 Tables: 0

27 Figures: 6

28 References: 36

29 Abstract word count: 208

30 Introduction word count: 723

31 Discussion word count: 988

32

Abstract

34 The TASK-3 channel is a member of the K2P family that is important for the maintenance

35 of the resting membrane potential. Previous studies have demonstrated that the TASK-3

36 channel is involved in several physiological and pathological processes, including

37 sleep/wake control, cognition and epilepsy. However, there is still a lack of selective

38 pharmacological tools for TASK-3, which limits further research on channel function. In this

39 work, using a high-throughput screen (HTS), we discovered that N-(2-((4-nitro-2-

40 (trifluoromethyl)phenyl)amino)ethyl)benzamide (NPBA) showed excellent potency and

41 selectivity as a novel TASK-3 activator. The molecular determinants of NPBA activation

42 were then investigated by combining chimera and mutagenesis analysis. Two distant

43 clusters of residues located at the extracellular end of the second transmembrane domain

44 (TM2) (A105 and A108) and the intracellular end of the third transmembrane domain (TM3)

45 (E157) were found to be critical for NPBA activation. We then compared the essentials of

46 the actions of NPBA with inhalation anesthetics that nonselectively activate TASK-3 and

47 found that they may activate TASK-3 channels through different mechanisms. Finally, the

48 three residues A105, A108 and E157 were transplanted into the TASK-1 channel, which

49 resists NPBA activation, and the constructed mutant TASK-1(G105A, V108A, A157E)

50 showed dramatically increased activation by NPBA, which confirms the importance of

51 these two distant clusters of residues.

MOL # 115303

Introduction

53   K2P channels conduct "leak" potassium currents, which play critical roles in the

54   maintenance of the resting membrane potential. The K2P family currently has 15

55   mammalian members, which can be divided into six distinct subfamilies based on structure

56   and functional properties. The TWIK-related acid-sensitive K (TASK)-3 channel is a

57   member of the K2P family and belongs to the TASK subfamily consisting of TASK-3, TASK-

58   1, and TASK-5 (Enyedi and Czirjak, 2010). TASK-3 and TASK-1 are functional channels

59   conducting currents highly sensitive to extracellular pH (Duprat et al., 1997; Kim et al.,

60   2000; Rajan et al., 2000), while TASK-5 cannot be functionally expressed (Kim and

61   Gnatenco, 2001).

62   Mainly expressed in the CNS, particularly in the cerebellum, hypothalamus and cortex

63   (Talley et al., 2001), TASK-3 was proposed to be related to mood disorders, sleep/wake

64   control and cognition (Gotter et al., 2011; Linden et al., 2007). The human TASK-3 mutation

65   G236R has been identified as responsible for mental retardation associated with a rare

66   maternally transmitted dysmorphism syndrome (Barel et al., 2008), and TASK-3 knock-out

67   mice showed impaired working memory and altered circadian rhythms (Linden et al., 2007).

68   Abundant TASK-3 expression was also found in the adrenal cortex, and it has been

69   demonstrated that TASK-3 channel deletion in mice could recapitulate low-renin essential

70   hypertension (Guagliardo et al., 2012). In addition, TASK-3 has been implicated in other

71   disorders, including cancer (Mu et al., 2003), primary hyperaldosteronism (Davies et al.,

72   2008), and epilepsy (Holter et al., 2005).

73 The TASK-3 channel, which is involved in multiple physiological and pathological

74 processes, can be modulated by various endogenous neurochemicals, clinically active

75 drugs, and physicochemical factors (Goldstein et al., 2001; Lesage, 2003; Talley et al.,

76 2003). The TASK-3 channel is closed by extracellular acidification (Duprat et al., 1997; Kim

77 et al., 2000; Rajan et al., 2000), and it is also inhibited by hormones and transmitters

78 through GPCRs (Chemin et al., 2003; Mathie, 2007; Talley and Bayliss, 2002); this

79 inhibition is now considered to be mediated by diacylglycerol (DAG) (Wilke et al., 2014).

80 Moreover, the TASK-3 channel is an important target of inhalation anesthetics such as

81 chloroform and respiratory stimulants such as doxapram (Cotten et al., 2006). In addition,

82 the TASK-3 channel is sensitive to other small-molecule compounds, such as ruthenium

83 red (Czirjak and Enyedi, 2002), anandamide (Berg et al., 2004), lidocaine (Kim et al., 2000)

84 and bupivacaine (Meadows and Randall, 2001). However, all the small-molecule regulators

85 above are nonselective, which limits their use as selective pharmacological tools for

86 research on TASK-3. Currently, the only reported selective activator of TASK-3 is

87 terbinafine, which has moderate potency with a maximum effect of ~ 2-fold and a pEC_{50} of

88 6.2 μM in the thallium flux assay, but the mechanism of action of this compound remains

89 unknown (Wright et al., 2017).

90 In mechanistic research on TASK-3 activators, the mechanism of action of inhalation

91 anesthetics on TASK-3 channels has been extensively studied and partially revealed.

92 Specifically, M159, a residue located on the cytoplasmic side of TM3, was proposed to be

93 the potential binding site of inhalation anesthetics (Andres-Enguix et al., 2007), and the

94 reliability of this conclusion was further evidenced by a later study using cysteine

95 modification (Conway and Cotten, 2012). In addition, amino acids 243 to 248 (VLRFLT),

96 located in the junction of TM4 and the carboxyl terminus (Ct), were also identified as

97 essential for activation by inhalation anesthetics (Patel et al., 1999), and this region was

98 also demonstrated to be important for the regulation of GPCR or other intracellular factors

99 (Talley and Bayliss, 2002). Several studies on TREK-1 (K_{2P}2.1) concluded that the TM4–

100 Ct junction was critical for the conduction of conformational transmission from the Ct to the

101 pore of the channel, which could be disturbed by a triple glycine mutation K_{2P}2.1-3G

102 (Bagriantsev et al., 2012; Bagriantsev et al., 2011). The up and down states of TM4 have

103 been proven to represent different conductive states that involve the conformational

104 transmission (Dong et al., 2015).

105 In this study, we searched for better small-molecule activators of TASK-3 by high-

106 throughput screening (HTS) and identified NPBA as a novel selective agonist of the TASK-

107 3 channel. Furthermore, by adopting various mutagenesis analyses, we found three

108 residues, A108, A105 and E157 that were important for NPBA activation. In addition, we

109 found that the selective activator we identified shared some common key residues with

110 inhalation anesthetics but may conduct channel activation through a different mechanism.

111 ## Materials and Methods

112 ### Plasmid construction

113 Human TASK-3, human TASK-1, and human TRESK were gifts from Dr Min Li (Johns

6

114 Hopkins University, USA). EGFP, human TREK-1 and rat THIK1 were provided by Jia Li

115 (Shanghai Institute of Materia Medica, China), Yang Li (Shanghai Institute of Materia

116 Medica, China) and Haijun Chen (State University of New York, USA). Point mutations of

117 TASK channels were introduced using the QuikChange II Site-directed Mutagenesis Kit

118 (Stratagene), and chimeras of the TASK channel were constructed using the In-Fusion HD

119 Cloning Kit (TaKaRa). All constructs were verified by sequencing.

120 **Cell culture and transient transfection**

121 CHO-K1 cells were cultured in DMEM/F12 (Gibco) with 10% FBS (Gibco). Twenty-four

122 hours prior to transfection, the cells were split into 6-well dishes. Plasmids encoding the

123 EGFP and K2P channels were cotransfected with Lipofectamine 3000 reagent (Invitrogen)

124 according to the manufacturer's instructions.

125 **Electrophysiological recording**

126 To measure the currents of the K2P channels expressed in CHO-K1 cells, standard whole-

127 cell patch clamping experiments were performed at room temperature. Pipettes with

128 resistance ranging from 2.0 to 5.0 MΩ were pulled using borosilicate glass capillaries

129 (World Precision Instruments). During the recording process, constant perfusion of bath

130 solution was maintained using a BPS perfusion system (ALA Scientific). The pipette

131 solution contained the following: 145 mM KCl, 1 mM MgCl2, 5 mM EGTA, and 10 mM

132 HEPES (pH 7.3 with KOH). The bath solution contained the following: 140 mM NaCl, 5 mM

133 KCl, 2 mM CaCl2, 1 mM MgCl2, 10 mM glucose and 10 mM HEPES (pH 7.4 with NaOH).

134   The whole-cell currents were recorded using an EPC-10 amplifier (HEKA), and signals

135   were filtered at 2 kHz, digitized using a DigiData 1440A, and analyzed with pClamp 9.2

136   software (Molecular Devices). The series resistance was compensated by 60%.

137   **Homology Modeling**

138   The structures of the TASK-3 channel were constructed based on the crystal structures of

139   the TREK-2 channel (PDB code 4BW5 and 4XDJ, identity: 31%) by using Modeler (Sali

140   and Blundell, 1993), which are reported as the conductive and nonconductive states,

141   separately. Multiple sequence alignment was generated by using the Clustal Omega web

142   server (https://www.ebi.ac.uk/Tools/msa/clustalo).

143   **Statistics**

144   Patch-clamp data were processed using Clampfit 10.2 (Molecular Devices) and then

145   analyzed in GraphPad Prism 5 (GraphPad Software). Dose–response curves were fitted

146   with the Hill equation, $E = E_{max}/[1 - (EC50/C]P)$, where EC50 is the drug concentration

147   producing the half-maximum response. The data are shown as the means ± SEM, and the

148   significance was estimated using one-way ANOVA followed by Dunnett's post hoc test.

149   Statistical significance: * $P < 0.05$, ** $P < 0.01$, *** $P < 0.001$.

Results

Identification of NPBA as a selective TASK-3 activator

To address the lack of selective pharmacology tools for the TASK-3 channel, we developed

an HTS to discover selective small-molecule TASK-3 modulators. Before the HTS, HEK293

cell lines stably expressing human TASK-3 or its closest homologue TASK-1 were

established because selective active compounds for the TASK subfamily were more likely

to exhibit selectivity among the K_{2P} family. Then, the channel activity was measured by a

thallium flux assay as in the previous work (Yu et al., 2015; Yue et al., 2016).

Within the project, more than 300,000 compounds were screened, of which 1417

compounds were identified as TASK-3 activators. Among these active compounds, N-(2-

((4-nitro-2-(trifluoromethyl)phenyl)amino)ethyl)benzamide (NPBA) exhibited the best

potency for TASK-3 activation and showed good selectivity between TASK channels. Fig.

1A shows the molecular structure of NPBA.

To confirm the activation of NPBA and to estimate its potency, whole-cell patch clamp

recordings were performed. CHO-K1 cells transiently transfected with wild-type human

TASK-3 or other K2P channels were used for the recording, and we ran a voltage-ramp

protocol from -130 mV to 20 mV to obtain the I-V curve. The current at 0 mV was chosen

to measure the potency of NPBA toward different channels. For the dose-response curve

study, we tested concentrations of NPBA ranging from 0.1 μM to 30 μM, as the compound

9

169 cannot be completely dissolved at a higher concentration of 100 µM. NPBA showed

170 reversible dose-dependent activation of TASK-3 whole-cell currents with an EC_{50} of 6.7 µM,

171 and the currents were increased by up to ~6-fold at a concentration of 10 µM (Fig. 1, B

172 and C). We also investigated the effects of 10 µM NPBA on other $K_{2P}s$, including TASK-1,

173 TREK-1, TRESK and THIK-1, but no activation was detected in these channels (Fig. 1D),

174 suggesting excellent selectivity of NPBA towards TASK-3 channels. As the closest

175 homologue of TASK-3, TASK-1 was also tested in a dose-response curve study, and it was

176 reversibly inhibited by NPBA in a dose-dependent manner, with an IC_{50} of 7.5 µM (Fig. 1,

177 E and F). These results indicated that NPBA was a potent activator of the TASK-3 channel

178 and has good selectivity.

The A108 residue located at the extracellular end of TM2 is crucial for activation by NPBA

179 **The A108 residue located at the extracellular end of TM2 is crucial for**

180 **activation by NPBA**

181 To identify regions of the TASK-3 channel that are necessary for activation by NPBA,

182 TASK-3 and TASK-1 subunits were used to make chimeric constructs because they shared

183 highly homologous sequences but showed greatly different responses to NPBA.

184 Using In-Fusion cloning technology, we first replaced the N-terminus of TASK-3 with a

185 homologous sequence from TASK-1 and gradually extended the replaced region. We

186 constructed T1-85-T3, in which amino acids 1-85 of TASK-3 were replaced by the

187 corresponding part of TASK-1, and we constructed T1-131-T3, T1-169-T3 and T1-209-T3

188 in the same manner. Then, the effects of NPBA on these chimeras were tested at a

189   concentration of 10 µM. The first chimera, T1-85-T3, with the junction in the first pore

190   domain, retained the activation by NPBA (Fig. 2A), while the other chimeras with the

191   junction at or after position 131 in this series were not activated by NPBA (Fig. 2, B-D).

192   These results indicated that there were key NPBA determinants within amino acids 85-131.

193   A mutagenesis scan was then performed to investigate the critical residues in this region.

194   We tested the effects of swapping each of the amino acids that differed between TASK-3

195   and TASK-1 within section 85-131 (Fig. 2E). In the TASK-3 channel, these four amino acids

196   were individually replaced by those in the homologous sites of TASK-1. Among the four

197   TASK-3 mutations (Fig. 2E), A105G moderately impaired the activation by NPBA, and the

198   current was increased by ~3-fold under 10 µM NPBA (Figs. 2F and 4G), while A108V

199   completely abrogated the activation by NPBA and showed inhibition at 10 µM NPBA (Figs.

200   2G and 4G). However, the other two mutants, G102S and V115L showed an NPBA

201   phenotype that was indistinguishable from the wild type (Fig. 4G).

202   Since the alanine at position 108 (A108) seemed to be crucial for activation by NPBA, we

203   replaced this alanine with various other amino acids, including phenylalanine, leucine,

204   isoleucine, glycine, tyrosine, cysteine, and serine. Among all these A108 mutants, only

205   A108G or A108S showed current activation in response to by 10 µM NPBA, while all other

206   mutant showed the same current inhibition as A108V (Fig. 3A). Furthermore, we performed

207   alanine scanning mutagenesis within the residues around A108 and evaluated the

208   responses under 10 µM NPBA. Among the nine mutant channels, four mutations (T103A,

209   D104A, F109A, and M111A) eliminated activation by NPBA and showed current inhibition

11

210   by NPBA, while mutations of the remaining five residues (P101A, G102A, G106A, K107A,

211   and C110A) showed only a slight decrease in the activation degree resulting from NPBA

212   (Fig. 3B). Taken together, these findings suggested that the residues around A108 played

213   a crucial role in NPBA activation on the TASK-3 channel.

A TASK-1 mutant with alanine at position 108 resists NPBA activation

214

215   Since the TASK-3 mutant A108V showed a total loss of NPBA activation, we wondered

216   whether the corresponding TASK-1 mutant V108A would gain activation by NPBA. As

217   shown in Fig. 3C, however, TASK-1(V108A) could not be activated by 10 µM NPBA. A

218   double-mutant TASK-1 channel (G105A, V108A) was then constructed by introducing

219   G105A into TASK-1(V108A). We found that the newly constructed mutant channel was

220   also unable to be activated by NPBA (Fig. 3D). In contrast, it showed an inhibition similar

221   to that in the wild-type TASK-1 or TASK-1(V108A). These results implied that these

222   residues on TM2 were not the only determinants responsible for the different NPBA

223   phenotypes of TASK-1 and TASK-3.

The intracellular end of TM3 is important for NPBA activation

224

225   Based on the results above, we concluded that there should be other important residues

226   for NPBA activation in addition to A105 and A108. To identify these unknown determinants,

227   we constructed another series of chimeras. In this group of chimeras, the C-terminal of

228   TASK-3 was replaced by the homologous sequence of TASK-1, and the junction was

12

229   moved forward gradually. We constructed T3-240-T1 as the protein sequence after position

230   240 of TASK-3 was replaced by the corresponding section of TASK-1 and constructed T3-

231   209-T1, T3-169-T1 and T3-131-T1 in the same manner. We then tested the effects of

232   NPBA at a concentration of 10 µM. With the junction moving forward, T3-240-T1, T3-209-

233   T1, and T3-169-T1 could all be activated by NPBA (Fig. 4, A-C), while the last chimera T3-

234   131-T1 could not be activated significantly by 10 µM NPBA (Fig. 4D). These results

235   suggested that there were determinants for NPBA activation within section 131-169 in

236   addition to 85-131.

237   Next, we performed scanning mutagenesis within amino acids 131-169 of TASK-3, and 16

238   mutants were constructed and evaluated (Fig. 4, E and G). Among these mutations, the

239   mutation E157A weakened NPBA activation the most, and the mutant currents showed

240   only a 2-fold enhancement under 10 µM NPBA (Fig. 4F). There are also other mutations

241   that impaired the activation, such as M168I and K141H, which showed a moderate ~3-fold

242   current activation in response to 10 µM NPBA (Fig. 4G).

243   Since the glutamic acid at position 157 (E157) seems to be important for NPBA activation,

244   we further changed this negatively charged amino acid to negatively charged aspartic acid,

245   positively charged arginine or neutral glutamine and determined the effects of 10 µM NPBA

246   on these mutants. Both E157D and E157R showed the same NPBA phenotype as E157A,

247   with only a 2-fold current enhancement under 10 µM NPBA. However, the E157Q current

248   was activated by 10 µM NPBA as effectively the wild-type TASK-3 channel, showing 6-fold

249   activation under 10 µM NPBA (Fig. 5A). These results suggested that E157 is also an

250   important residue for NPBA activation, and the volume rather than the charge of the residue

251   at position 157 is the key characteristic necessary to achieve a potent activation by NPBA.

252   NPBA activates TASK-3 through a different mechanism from inhalation

253   anesthetics

254   E157 was predicted to be located in the intracellular end of TM3 on the basis of hydropathic

255   analysis (Kim et al., 2000) and is very close to M159 (Figs. 4E and 6G), a residue reported

256   to be the binding site of nonselective inhalation anesthetics. Thus, we wondered whether

257   activation by NPBA and activation by inhalation anesthetics occurred through a common

258   mechanism. In this study, chloroform was selected as a representative inhalation

259   anesthetic and increased the wild-type TASK-3 current approximately 2-fold at a

260   concentration of 5 mM (Fig. 5, B and J), which is consistent with previous results (Andres-

261   Enguix et al., 2007). Thereafter, we determined and compared the effects of NPBA and

262   chloroform on the mutant channels that have been reported to show impaired anesthetic

263   activation. First, we constructed the mutant   that showed increased basal currents and

264   resistance to activation by inhalation anesthetics (Conway and Cotten, 2012). M159W

265   completely abrogated the activation by 5 mM chloroform, while activation by NPBA was

266   partially retained (Fig. 5, C, D and J). Then, we constructed the mutant R245W with a large

267   tryptophan predicted to occupy the space around M159, similar to M159W (Fig. 6G).

268   Notably, this alteration abolished activation by both NPBA and chloroform and showed a

269   different NPBA phenotype from that of M159W (Fig. 5 E, F and J). In addition, we

270   constructed a TASK-3 mutant 242-3G with three residues, V242-V243-L244, replaced by

271 glycines, based on a $K_{2P}2.1$-3G mutant predicted to uncouple the cross-talk between the

272 pore and carboxyl terminus (Bagriantsev et al., 2012). Subsequently, 5 mM chloroform

273 failed to induce an increase in current in the 242-3G mutant and instead showed an

274 inhibitory effect on the current (Fig. 5, H and J), suggesting that this triple glycine mutation

275 also affects the TASK-3 channel. However, the activation by NPBA was retained in the 242-

276 3G mutant, with a potency of 2-fold under a concentration of 10 mM (Fig. 5, G and J).

277 Finally, we tested the effect of 5 mM chloroform on the A108V mutant that completely

278 abolished NPBA activation (Fig. 2G). The activation degree of 5 mM chloroform for A108V

279 was indistinguishable from that for the wild-type TASK-3 channel (Fig. 5, I and J). Taken

280 together, these results demonstrated that though activation by NPBA and inhalation

281 anesthetics shared some key residues, such as M159, they were likely to activate the

282 channel through different action mechanisms.

283 **A TASK-1 mutant with three key residues swapped gains NPBA activation**

284 Since the amino acids 131-169 were also shown to be vital regions for NPBA activation

285 and E157 seemed to be the most important residue in this region, we transplanted E157

286 into the mutant channel TASK-1(G105A,V108A) to construct the mutant TASK-1(G105A,

287 V108A, A157E), and then we determined the effect of 10 μM NPBA on this triple-mutant

288 channel. The logic here was to try to construct a TASK-1 mutant that could be activated by

289 NPBA to confirm the importance of these residues. Dramatically, TASK-1(G105A, V108A,

290 A157E) gained NPBA activation, and the current in the mutant showed a 1.5-fold increase

291 under a NPBA concentration of 10 μ M (Fig. 6, A and C). In contrast, a mutant with two

15

292   sites changed, TASK-1(V108A, A157E) did not gain activation by 10 μM NPBA (Fig. 6, B

293   and C). Notably, TASK-1(G105A, V108A, A157E) showed an NPBA phenotype combining

294   the responses of TASK-1 and TASK-3. After the administration of NPBA, the mutant

295   currents decreased initially for seconds and then increased gradually, displaying an inward

296   hook on the time course plot (Fig. 6A). We speculated that the intrinsic inhibition of TASK-

297   1 perhaps counteracts the acquired potentiation from the three mutations (G105A, V108A,

298   A157E), resulting in a weaker activation of the current amplitude than that of the wild-type

299   TASK-3 channel. These results demonstrated that A108, A105 and E157 were important

300   for activation (Fig. 6D).

301   Based on the crystal structures of TREK-2, we created an open-state homology model of

302   TASK-3 (Fig. 6E). Structurally, the key residues A105 and A108 lie at the extracellular end

303   of TM2, a pore-lining helix adjacent to P1 and P2 (Fig. 6, D-F), while the third key residue

304   E157 is located in the intracellular end of TM3 (Fig. 6, D, E and G). Notably, these two

305   regions are separated by a long distance of approximately 26.6 Å (Fig. 6E).

Discussion

307   Among K2P channels, the TASK-3 channel has been implicated in a number of normal

308   physiological processes or disorders, but few selective TASK-3 channel modulators have

309   been identified, which hinders the understanding of channel function in physiology.

310   Terbinafine, an antifungal medication, was the first and previously the only selective

311   activator of TASK-3 reported, but this compound only has a moderate activation effect. In

312   the present work, we identified NPBA as a novel agonist of the TASK-3 channel by HTS.

313   NPBA produces ~6-fold activation under a concentration of 10 µM (Fig. 1B) and is thus

314   more potent than terbinafine, though the EC_{50} of NPBA (6.7 µM) is almost equal to that

315   of terbinafine (6.2 µM) (Fig. 1C). In addition, NPBA also has good selectivity (Fig. 1C),

316   which makes it a useful pharmacological probe for in vitro studies of TASK-3 function and

317   in further studies intended for therapeutic intervention.

318   The study of the molecular mechanisms of modulators is an important aspect of ion

319   channel research. For TASK-3, previous studies mainly focused on the regulation of pH

320   and inhalation anesthetics. Though some explicit results have been obtained (Andres-

321   Enguix et al., 2007; Conway and Cotten, 2012), fewer novel elements in the activation

322   mechanism of TASK-3 have been reported in recent years, which may be due to the lack

323   of novel modulators of TASK-3. Adopting the classical chimera strategy and various

324   mutagenesis analyses in this work, we found several residues that are important for NPBA

325   activation, whose alteration could significantly impair NPBA activation (Figs. 2, 3 and 4).

326   By transplanting three of these residues, A105, A108 and E157, into the TASK-1 channel,

327   which resists activation by NPBA, the TASK-1 mutant TASK-1 (G105A, V108A, A157E)

328   was constructed and dramatically gained activation by NPBA (Fig. 6, A and C). This gain

329   of activation is more convincing because no binding assay or cocrystallization research

330   has been performed in previous studies of TASK-3, which further confirms the importance

331   of these residues. Among the three residues, A108 and A105 lie at the proximal

332   amphipathic end of TM2 adjacent to P1 and P2 (Fig. 6, D and F), which may be related to

17

333   selective filter gating, while E157 is spatially adjacent to the distal end of TM4, the up and

334   down states of which have been proven to represent different conductive states (Fig.

335   6G)(Dong et al., 2015). These residues have never been mentioned in previous studies of

336   TASK-3 and may provide clues for the understanding of the gate mechanism of TASK-3.

337   The mechanism of the activation of TASK-3 by inhalation anesthetics has been partially

338   revealed. The binding site of these molecules was believed to be located on the

339   intracellular side of TM3 near M159 (Andres-Enguix et al., 2007; Conway and Cotten,

340   2012). In addition, the amino acids 243-248 were also involved in the inhalation anesthetic

341   activation (Talley and Bayliss, 2002). In the present work, by comparing the phenotypes of

342   the response to NPBA and chloroform in multiple TASK-3 mutants, we found that some

343   mutants, such as R245W, affected activations by both NPBA and chloroform (Fig. 5 E and

344   F). However, the elements that are vital for the activation of NPBA and chloroform did not

345   overlap perfectly. Specifically, the most crucial mutant for NPBA activation, A108V, did not

346   change the chloroform activation (Figs. 2G and 5I); the mutant 242-3G retained NPBA

347   activation, although chloroform activation was abolished (Fig. 5, G and H). Among the

348   mutations that weakened the activation by chloroform, M159W is a classic mutation that

349   has proven to be effective by occupying the space around the binding site of chloroform

350   with a tryptophan and mimicking a chloroform-bound more conductive conformation.

351   Interestingly, R245W seems to affect the activation of chloroform in a similar manner since

352   R245 is spatially near M159. However, NPBA activation was partially retained in M159W,

353   suggesting that NPBA does not share M159 as a binding site with chloroform. Accordingly,

354   the activation effect of NPBA on wild-type TASK3 was tested in the presence of 10 mM

355   chloroform, a saturated concentration of the inhalation anesthetic. We found that NPBA

356   further significantly potentiated the increased currents by chloroform (Supplementary Fig.

357   2). These results suggest that the novel activator NPBA may activate TASK-3 differently

358   from inhalation anesthetics.

359   The TM4 and Ct domains in K2Ps have proven to be important regions for a range of

360   signaling inputs within the cell, including temperature (Maingret et al., 2000), mechanical

361   force (Patel et al., 1998), and phosphorylation (Bagriantsev et al., 2012). Notably, the

362   crosstalk between the two regions can be broken by the 242-3G mutation (Bagriantsev et

363   al., 2012). In our work, the 242-3G mutation completely abolished the activation by

364   chloroform, which could be explained by the fact that activation by chloroform depends on

365   the relay from the Ct domain to TM4 or that this 3G mutation causes conformational

366   changes in the anesthetic pocket. However, NPBA activation was retained in 242-3G,

367   indicating that the binding site of NPBA is upstream of the link between TM4 and the Ct

368   domain. Finally, A108, a brand new residue we identified, was found to be necessary only

369   for activation by NPBA rather than chloroform. Because mutating 3 residues (G105A,

370   V108A, and A157E) in TASK-1 partially conferred NPBA activation on TASK-1, we

371   speculated that a long-range coupling between the extracellular segment around A108 and

372   the intracellular domains around E157 might be involved in NPBA-induced activation. To

373   elucidate the specific mechanism underlying potential cooperation, further studies, such as

374   binding assays, computational simulations and crystallization research, are necessary.

375   In conclusion, we have described the ability of a novel compound, NPBA, to activate the

376   TASK-3 channel. This compound also displays marked specificity within the K2P group

377   and may therefore be a good pharmacological tool for TASK-3 research. Several additional

378   elements that are important for NPBA action have also been uncovered in our work. This

379   finding provides a strategy to identify more novel TASK-3 activators, and the key residues

380   we found, such as A108, may promote research on the gate mechanism of K_{2P} channels.

381

382   ## Author Contributions

383   Research design: Gao

384   Conducted experiments: Tian, Lan,

385   Performed data analysis: Tian, Lan, Qiu, Li and Yang

386   Wrote the manuscript: Tian, Gao

387   ## References

388   Andres-Enguix I, Caley A, Yustos R, Schumacher MA, Spanu PD, Dickinson R, Maze M and Franks NP
389   (2007) Determinants of the anesthetic sensitivity of two-pore domain acid-sensitive
390   potassium channels: molecular cloning of an anesthetic-activated potassium channel from
391   Lymnaea stagnalis. *The Journal of biological chemistry* **282**:20977-20990.
392   Bagriantsev SN, Clark KA and Minor DL, Jr. (2012) Metabolic and thermal stimuli control K(2P)2.1
393   (TREK-1) through modular sensory and gating domains. *The EMBO journal* **31**:3297-3308.
394   Bagriantsev SN, Peyronnet R, Clark KA, Honore E and Minor DL, Jr. (2011) Multiple modalities converge
395   on a common gate to control K2P channel function. *The EMBO journal* **30**:3594-3606.
396   Barel O, Shalev SA, Ofir R, Cohen A, Zlotogora J, Shorer Z, Mazor G, Finer G, Khateeb S, Zilberberg N
397   and Birk OS (2008) Maternally inherited Birk Barel mental retardation dysmorphism

398   syndrome caused by a mutation in the genomically imprinted potassium channel KCNK9.
399   *American journal of human genetics* **83**:193-199.

400   Berg AP, Talley EM, Manger JP and Bayliss DA (2004) Motoneurons express heteromeric TWIK-related
401   acid-sensitive K+ (TASK) channels containing TASK-1 (KCNK3) and TASK-3 (KCNK9) subunits.
402   *The Journal of neuroscience : the official journal of the Society for Neuroscience* **24**:6693-
403   6702.

404   Chemin J, Girard C, Duprat F, Lesage F, Romey G and Lazdunski M (2003) Mechanisms underlying
405   excitatory effects of group I metabotropic glutamate receptors via inhibition of 2P domain K+
406   channels. *The EMBO journal* **22**:5403-5411.

407   Conway KE and Cotten JF (2012) Covalent modification of a volatile anesthetic regulatory site activates
408   TASK-3 (KCNK9) tandem-pore potassium channels. *Molecular pharmacology* **81**:393-400.

409   Cotten JF, Keshavaprasad B, Laster MJ, Eger EI, 2nd and Yost CS (2006) The ventilatory stimulant
410   doxapram inhibits TASK tandem pore (K2P) potassium channel function but does not affect
411   minimum alveolar anesthetic concentration. *Anesthesia and analgesia* **102**:779-785.

412   Czirjak G and Enyedi P (2002) Formation of functional heterodimers between the TASK-1 and TASK-3
413   two-pore domain potassium channel subunits. *The Journal of biological chemistry* **277**:5426-
414   5432.

415   Davies LA, Hu C, Guagliardo NA, Sen N, Chen X, Talley EM, Carey RM, Bayliss DA and Barrett PQ (2008)
416   TASK channel deletion in mice causes primary hyperaldosteronism. *Proceedings of the*
417   *National Academy of Sciences of the United States of America* **105**:2203-2208.

418   Dong YY, Pike AC, Mackenzie A, McClenaghan C, Aryal P, Dong L, Quigley A, Grieben M, Goubin S,
419   Mukhopadhyay S, Ruda GF, Clausen MV, Cao L, Brennan PE, Burgess-Brown NA, Sansom MS,
420   Tucker SJ and Carpenter EP (2015) K2P channel gating mechanisms revealed by structures of
421   TREK-2 and a complex with Prozac. *Science* **347**:1256-1259.

422   Duprat F, Lesage F, Fink M, Reyes R, Heurteaux C and Lazdunski M (1997) TASK, a human background
423   K+ channel to sense external pH variations near physiological pH. *The EMBO journal* **16**:5464-
424   5471.

425   Enyedi P and Czirjak G (2010) Molecular background of leak K+ currents: two-pore domain potassium
426   channels. *Physiological reviews* **90**:559-605.

427   Goldstein SA, Bockenhauer D, O'Kelly I and Zilberberg N (2001) Potassium leak channels and the KCNK
428   family of two-P-domain subunits. *Nature reviews Neuroscience* **2**:175-184.

429   Gotter AL, Santarelli VP, Doran SM, Tannenbaum PL, Kraus RL, Rosahl TW, Meziane H, Montial M, Reiss
430   DR, Wessner K, McCampbell A, Stevens J, Brunner JI, Fox SV, Uebele VN, Bayliss DA, Winrow
431   CJ and Renger JJ (2011) TASK-3 as a potential antidepressant target. *Brain research* **1416**:69-
432   79.

433   Guagliardo NA, Yao J, Hu C, Schertz EM, Tyson DA, Carey RM, Bayliss DA and Barrett PQ (2012) TASK-3
434   channel deletion in mice recapitulates low-renin essential hypertension. *Hypertension*
435   **59**:999-1005.

436   Holter J, Carter D, Leresche N, Crunelli V and Vincent P (2005) A TASK3 channel (KCNK9) mutation in a
437   genetic model of absence epilepsy. *Journal of molecular neuroscience : MN* **25**:37-51.

438   Kim D and Gnatenco C (2001) TASK-5, a new member of the tandem-pore K(+) channel family.
439   *Biochemical and biophysical research communications* **284**:923-930.

440   Kim Y, Bang H and Kim D (2000) TASK-3, a new member of the tandem pore K(+) channel family. *The*
441   *Journal of biological chemistry* **275**:9340-9347.

21

MOL # 115303

442   Lesage F (2003) Pharmacology of neuronal background potassium channels. *Neuropharmacology*
443   **44**:1-7.

444   Linden AM, Sandu C, Aller MI, Vekovischeva OY, Rosenberg PH, Wisden W and Korpi ER (2007) TASK-3
445   knockout mice exhibit exaggerated nocturnal activity, impairments in cognitive functions, and
446   reduced sensitivity to inhalation anesthetics. *The Journal of pharmacology and experimental*
447   *therapeutics* **323**:924-934.

448   Maingret F, Lauritzen I, Patel AJ, Heurteaux C, Reyes R, Lesage F, Lazdunski M and Honore E (2000)
449   TREK-1 is a heat-activated background K(+) channel. *The EMBO journal* **19**:2483-2491.

450   Mathie A (2007) Neuronal two-pore-domain potassium channels and their regulation by G protein-
451   coupled receptors. *The Journal of physiology* **578**:377-385.

452   Meadows HJ and Randall AD (2001) Functional characterisation of human TASK-3, an acid-sensitive
453   two-pore domain potassium channel. *Neuropharmacology* **40**:551-559.

454   Mu D, Chen L, Zhang X, See LH, Koch CM, Yen C, Tong JJ, Spiegel L, Nguyen KC, Servoss A, Peng Y, Pei L,
455   Marks JR, Lowe S, Hoey T, Jan LY, McCombie WR, Wigler MH and Powers S (2003) Genomic
456   amplification and oncogenic properties of the KCNK9 potassium channel gene. *Cancer cell*
457   **3**:297-302.

458   Patel AJ, Honore E, Lesage F, Fink M, Romey G and Lazdunski M (1999) Inhalational anesthetics
459   activate two-pore-domain background K+ channels. *Nature neuroscience* **2**:422-426.

460   Patel AJ, Honore E, Maingret F, Lesage F, Fink M, Duprat F and Lazdunski M (1998) A mammalian two
461   pore domain mechano-gated S-like K+ channel. *The EMBO journal* **17**:4283-4290.

462   Rajan S, Wischmeyer E, Xin Liu G, Preisig-Muller R, Daut J, Karschin A and Derst C (2000) TASK-3, a
463   novel tandem pore domain acid-sensitive K+ channel. An extracellular histiding as pH sensor.
464   *The Journal of biological chemistry* **275**:16650-16657.

465   Sali A and Blundell TL (1993) Comparative protein modelling by satisfaction of spatial restraints.
466   *Journal of molecular biology* **234**:779-815.

467   Talley EM and Bayliss DA (2002) Modulation of TASK-1 (Kcnk3) and TASK-3 (Kcnk9) potassium
468   channels: volatile anesthetics and neurotransmitters share a molecular site of action. *The*
469   *Journal of biological chemistry* **277**:17733-17742.

470   Talley EM, Sirois JE, Lei Q and Bayliss DA (2003) Two-pore-Domain (KCNK) potassium channels:
471   dynamic roles in neuronal function. *The Neuroscientist : a review journal bringing*
472   *neurobiology, neurology and psychiatry* **9**:46-56.

473   Talley EM, Solorzano G, Lei Q, Kim D and Bayliss DA (2001) Cns distribution of members of the two-
474   pore-domain (KCNK) potassium channel family. *The Journal of neuroscience : the official*
475   *journal of the Society for Neuroscience* **21**:7491-7505.

476   Wilke BU, Lindner M, Greifenberg L, Albus A, Kronimus Y, Bunemann M, Leitner MG and Oliver D
477   (2014) Diacylglycerol mediates regulation of TASK potassium channels by Gq-coupled
478   receptors. *Nature communications* **5**:5540.

479   Wright PD, Veale EL, McCoull D, Tickle DC, Large JM, Ococks E, Gothard G, Kettleborough C, Mathie A
480   and Jerman J (2017) Terbinafine is a novel and selective activator of the two-pore domain
481   potassium channel TASK3. *Biochemical and biophysical research communications* **493**:444-
482   450.

483   Yu H, Zou B, Wang X and Li M (2015) Effect of tyrphostin AG879 on Kv 4.2 and Kv 4.3 potassium
484   channels. *British journal of pharmacology* **172**:3370-3382.

485   Yue JF, Qiao GH, Liu N, Nan FJ and Gao ZB (2016) Novel KCNQ2 channel activators discovered using

22

486   fluorescence-based and automated patch-clamp-based high-throughput screening

487   techniques. *Acta pharmacologica Sinica* **37**:105-110.

Footnotes

Figure Legends

494 **Figure 1. NPBA selectively activates TASK-3 channel in a dose-depend**

495 **manner.**

496 **(A)** Chemical structure of NPBA.

497 **(B)** Typical whole-cell current traces recorded from CHO-K1 cells overexpressing the

498   TASK-3 channel with normal bath solution or that with 10 µM NPBA. Currents at 0 mV

499   was plotted over time to reveal changes in response to NPBA. Period with NPBA

500   administration is marked by an orange bar and circle filled with orange, while circles

501   filled with blue shown currents with normal bath solution administration. Another

502   version of typical traces and timecourse with complete washout phase was shown in

503   Supplementary Fig 1.

504   **(C)** Dose-dependent curve of NPBA on TASK-3 channel. Each point represents the mean

505   with bars of S.E.M (n > 6).

506   **(D)** The statistics of the activation of 10 µM or 30 µM NPBA for TASK-3, TASK-1, TREK-1,

507   TRESK, and THIK-1 channels showing differences in NPBA sensitivity, with effects of

508   10 µM shown in orange while effects of 30 µM shown in red.

509   **(E)** Typical whole-cell current traces recorded from CHO-K1 cells overexpressing the

510   TASK-1 channel with normal bath solution or that with 10 µM NPBA.

511   **(F)** Dose-dependent curve of NPBA on TASK-1 channel. Each point represents the mean

512   with bars of S.E.M (n > 4).

513   **Figure 2. Segment 85-131 is important for TASK-3 activation.**

514   **(A-D)** Typical whole-cell current traces and time courses recorded from CHO-K1 cells

515   overexpressing the T1-85-T3 **(A)**, T1-131-T3 **(B)**, T1-169-T3 **(C)**, or T1-240-T3 **(D)** mutant

516   channel with 10 µM NPBA. Protein secondary structure of chimera is shown beside the

517   current traces, and section of TASK-3 appears in orange while section of TASK-1 appears

518   in blue.

519   **(E)** Sequence alignment of TASK-3 and TASK-1 for the residues 85-131. Residues different

520   in TASK channels appear in jacinth. The pore domain and TM2 are marked above the

521   sequences. Residues revealed important in swapping mutagenesis are marked with

522   arrows.

523   **(F and G)** Typical whole-cell current traces and time courses recorded from CHO-K1 cells

524   overexpressing the TASK-3(A105G) **(F)** or TASK-3(A108V) **(G)** mutant with 10 μM NPBA.

525   **Figure 3. Residues around A108 is important for NPBA activation.**

526   **(A)** The statistics of the activation of 10μM NPBA for wild-type TASK-3 (n=10), A108G

527   (n=4), A108S (n=4), A108C (n=4), A108V (n=7), A108L (n=4), A108I (n=4), A108F

528   (n=4), and A108Y (n=4).

529   **(B)** The statistics of the activation of 10μM NPBA for wild-type TASK-3 (n=10), P101A (n=4),

530   T103A (n=5), D104A (n=5), G106A (n=4), K107A (n=6), F109A (n=4), C110A (n=4),

531   and M111A (n=5), with activation effects shown in orange while inhibition effects shown

532   in blue.

533   **(C and D)** Typical whole-cell current traces and time courses recorded from CHO-K1 cells

534   overexpressing the TASK-1(V108A) **(C)** or TASK-1(V108A, G105A) **(D)** mutant with 10 μM

535   NPBA.

536   **Figure 4. Segment 131-169 is important for NPBA activation.**

537   **(A-D)** Typical whole-cell current traces and time courses recorded from CHO-K1 cells

538   overexpressing the T3-240-T1 **(A)**, T3-169-T1 **(B)**, T3-131-T1 **(C)**, or T3-85-T1 **(D)** mutant

539   channel with 10 μM NPBA. Protein secondary structure of chimera is shown beside the

540   current traces, and section of TASK-3 appears in orange while section of TASK-1 appears

541   in blue.

542   **(E)** Sequence alignment of TASK-3 and TASK-1 for the residues 131-169. Residues

543   different in TASK channels appear in jacinth. The TM3 is marked above the sequences.

544   Residues revealed important in swapping mutagenesis are marked with arrows.

545   **(F)** Typical whole-cell current traces and time courses recorded from CHO-K1 cells

546   overexpressing the TASK-3(E157A) mutant with 10 μM NPBA.

547   **(G)** Histograms summarizing the activation of 10μM NPBA for wild-type TASK-3 and TASK-

548   3 mutants with substitution of TASK-1 residues within 85-131 or 131-169, with activation

549   effects shown in orange while inhibition effects shown in blue. A108V is the only mutant

550   showing a final inhibition with 10μM NPBA. The baseline and NPBA peak-activated current

551   values and the I/I0 of TASK-3 mutants was shown in Supplemental Table 1.

552   **Figure 5. Activations by NPBA and chloroform have different**

553   **determinants.**

554   **(A)** The statistics of the activation of 10μM NPBA for wild-type TASK-3 (n=10), E157Q

555   (n=4), E157D (n=5), and E157R (n=5). The activation of NPBA on TASK-3 mutants were

556   compared to wild-type, statistical significance: * $P < 0.05$, ** $P < 0.01$, *** $P < 0.001$.

557 **(B)** Typical whole-cell current traces and time courses recorded from CHO-K1 cells

558 overexpressing TASK-3 channel with 5 mM chloroform.

559 **(C and D)** Typical whole-cell current traces and time courses recorded from CHO-K1 cells

560 overexpressing the TASK-3(M159W) mutant with 10 µM NPBA **(C)** or 5 mM chloroform

561 **(E and F)** Typical whole-cell current traces and time courses recorded from CHO-K1 cells

562 overexpressing the TASK-3(R245W) mutant with 10 µM NPBA **(E)** or 5 mM chloroform

563 **(G and H)** Typical whole-cell current traces and time courses recorded from CHO-K1 cells

564 overexpressing the 242-3G mutant with 10 µM NPBA **(G)** or 5 mM chloroform **(H)**.

565 **(I)** Typical whole-cell current traces and time courses recorded from CHO-K1 cells

566 overexpressing the A108V mutant with 5 mM chloroform. Magenta trace, current under 5

567 mM chloroform; blue trace, current under normal bath solution. Period with chloroform

568 administration is marked by a magenta bar and circle filled with magenta, while circles filled

569 with blue shown currents with normal bath solution administration.

570 **(J)** Histograms summarizing the activation of 10µM NPBA or 5 mM chloroform for wild-type

571 TASK-3, M159W, R245W, 242-3G, and A108V, with NPBA effects shown in bars filled with

572 orange while chloroform shown with bars filled with magenta. n= 4-10.

573   **Figure 6. A TASK-1 mutant gains the activation by NPBA after A105, A108**

574   **and E157 transplanted into.**

575   **(A and B)** Typical whole-cell current traces and time courses recorded from CHO-K1 cells

576   overexpressing TASK-1(V108A, G105A, A157E) **(A)** and TASK-1(V108A, A157E) **(B)**

577   channel with 10 μM NPBA.

578   **(C)** Histograms summarizing the activation of 10μM NPBA TASK-1(V108A, G105A, A157E)

579   (n=8), TASK-1(V108A, A157E) (n=6) and TASK-1(V108A, G105A) (n=5).

580   **(D)** Important residues for NPBA activation in a topology of TASK-3 subunit.

581   **(E)** Homology model of TASK-3 channel. Crucial residues A105, A108 and E157 for NPBA

582   activation are shown in yellow spheres.

583   （**F)** Top view of TMs and filter domain, the important residues on one TM2 subunit are

584   labeled.

585   **(G)** Detailed view of protein domains around E157. The putative anesthetic binding pocket

586   is shown in purple spheres. The up and down states of distal end of TM4 are represented

587   by $TM4^U$ and $TM4^D$ separately.
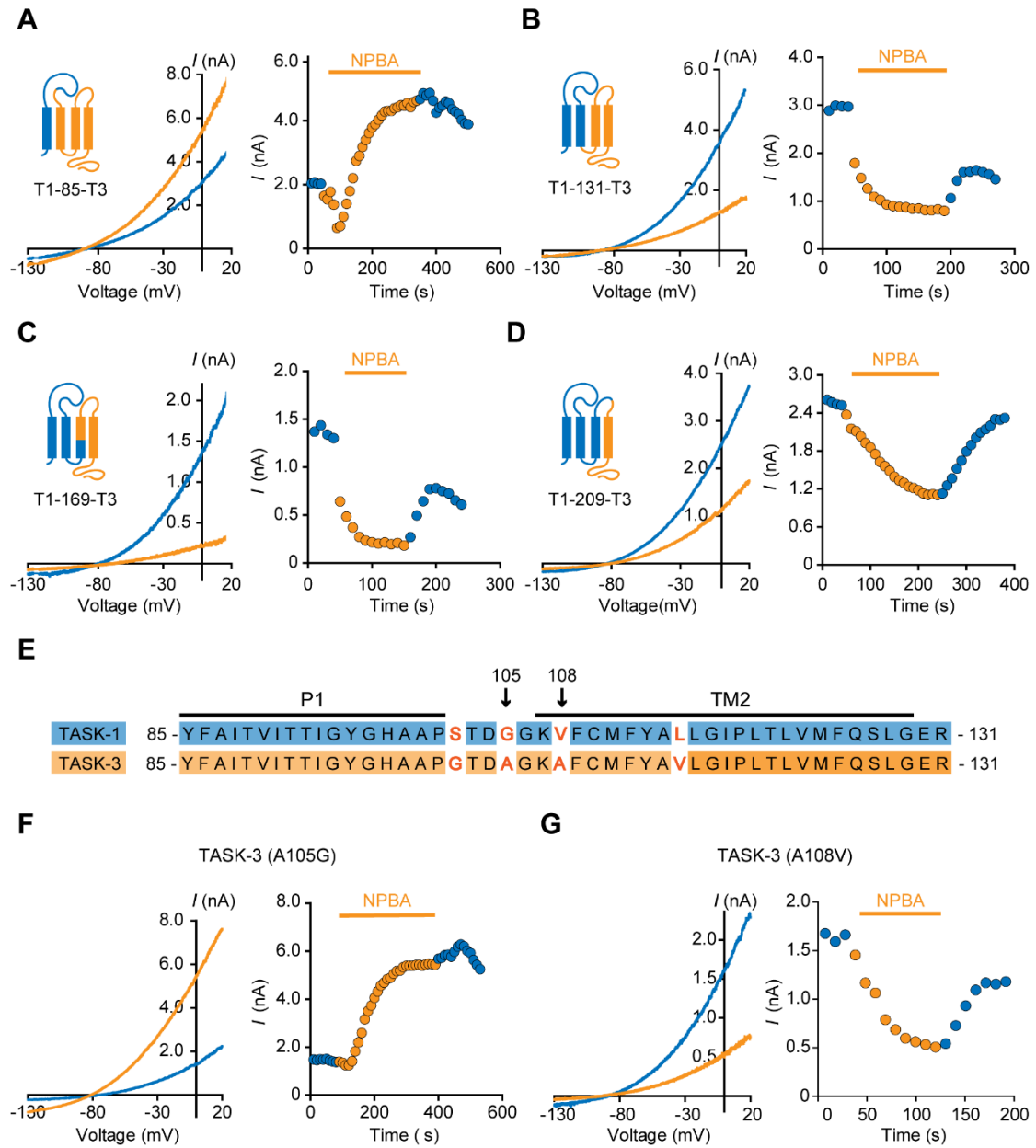
588   **Figures (6)**
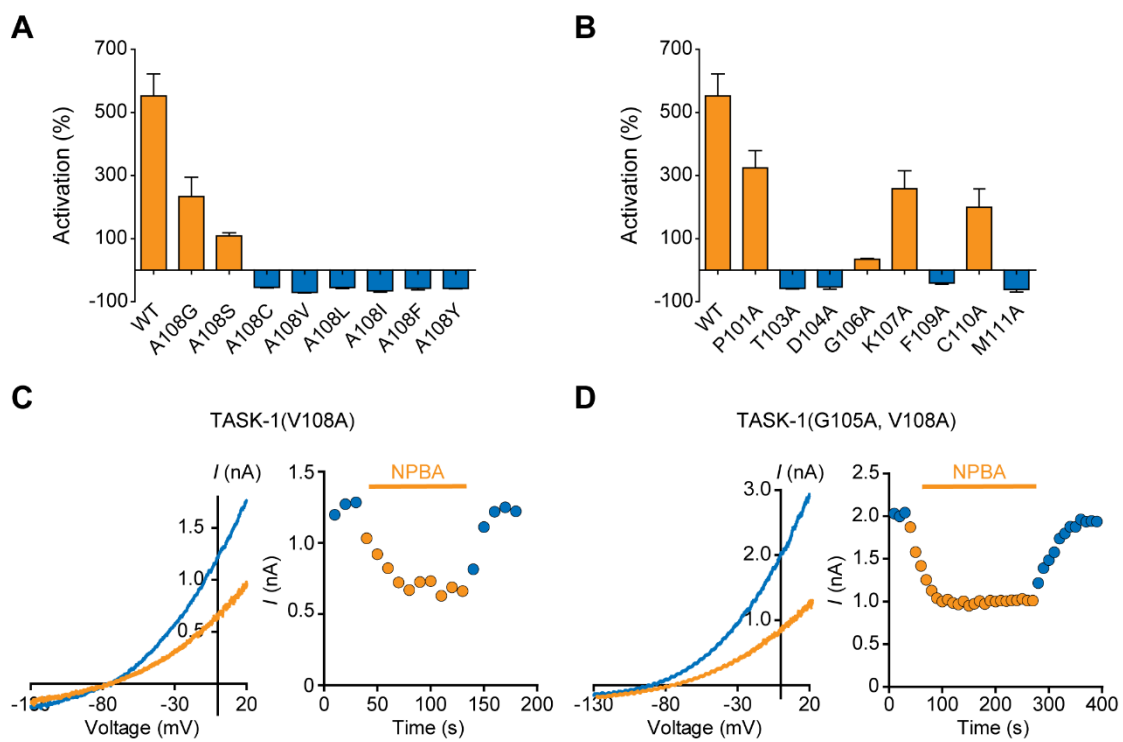
589   Figure 1
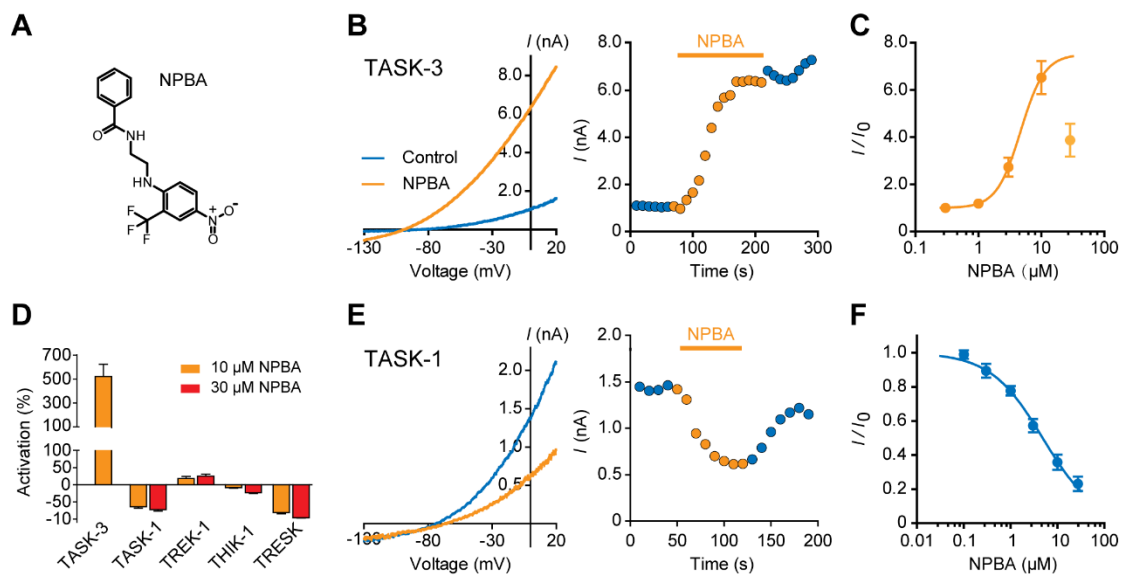
590

591

592

593   Figure 2

594

595

596   Figure 3
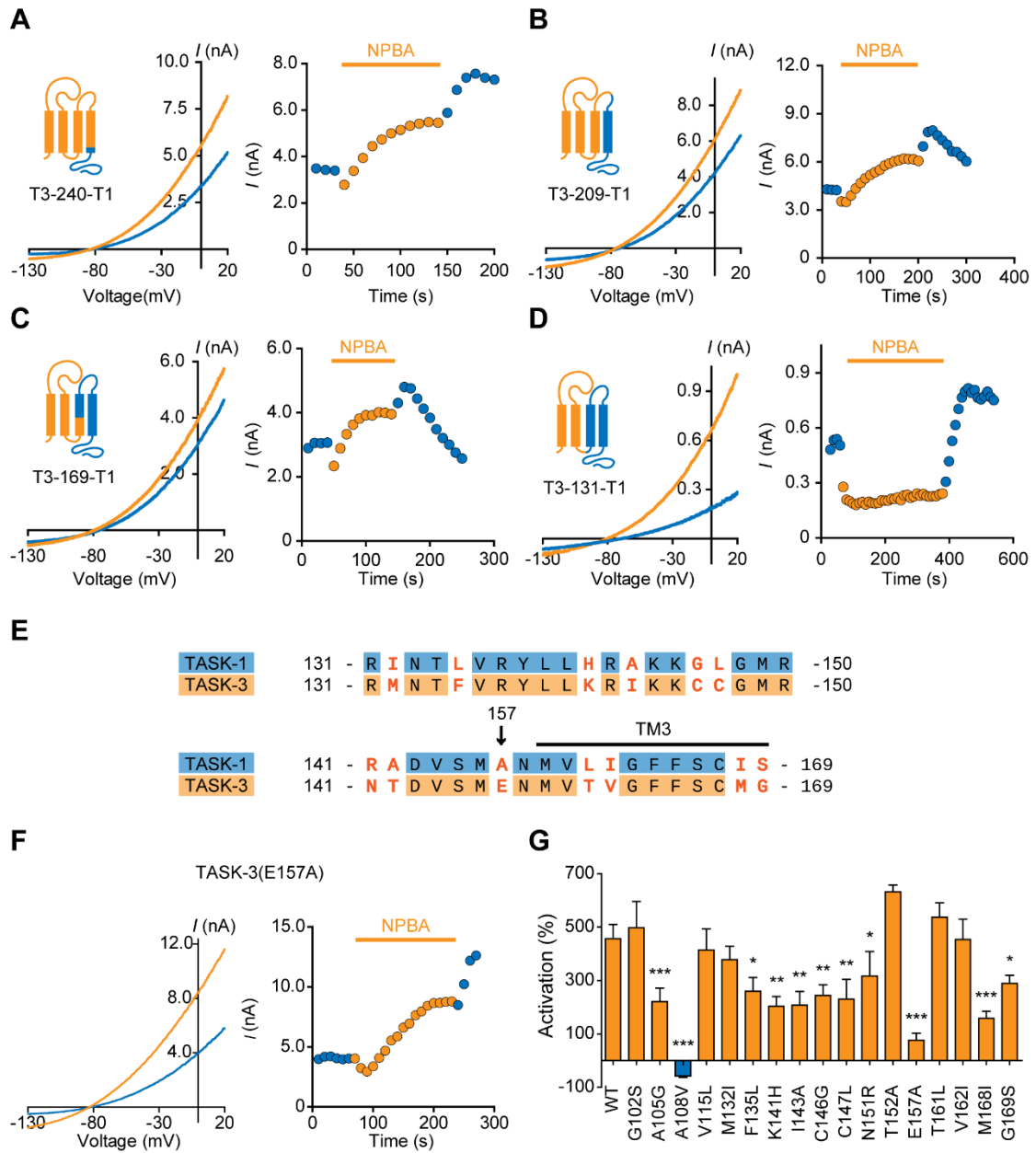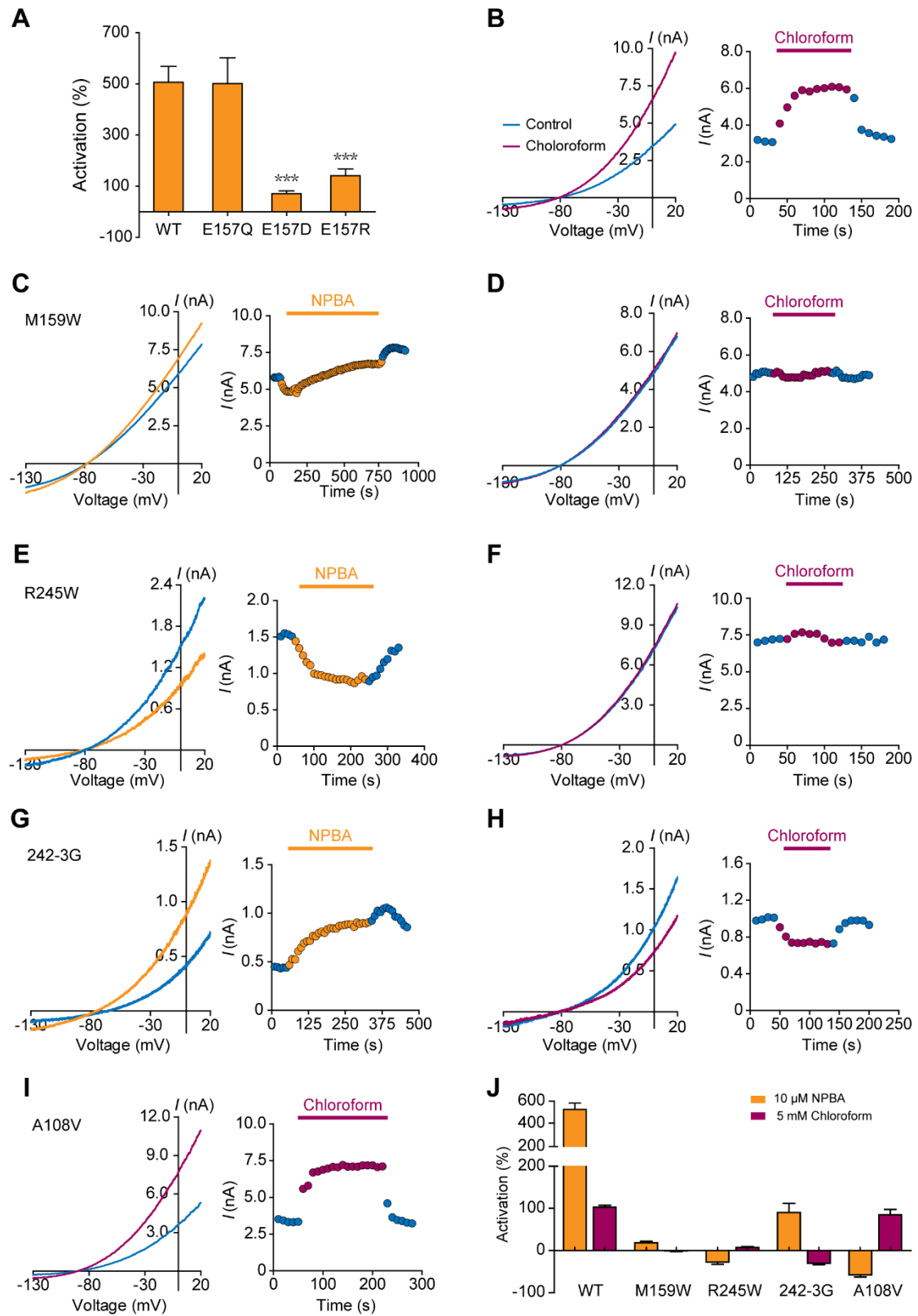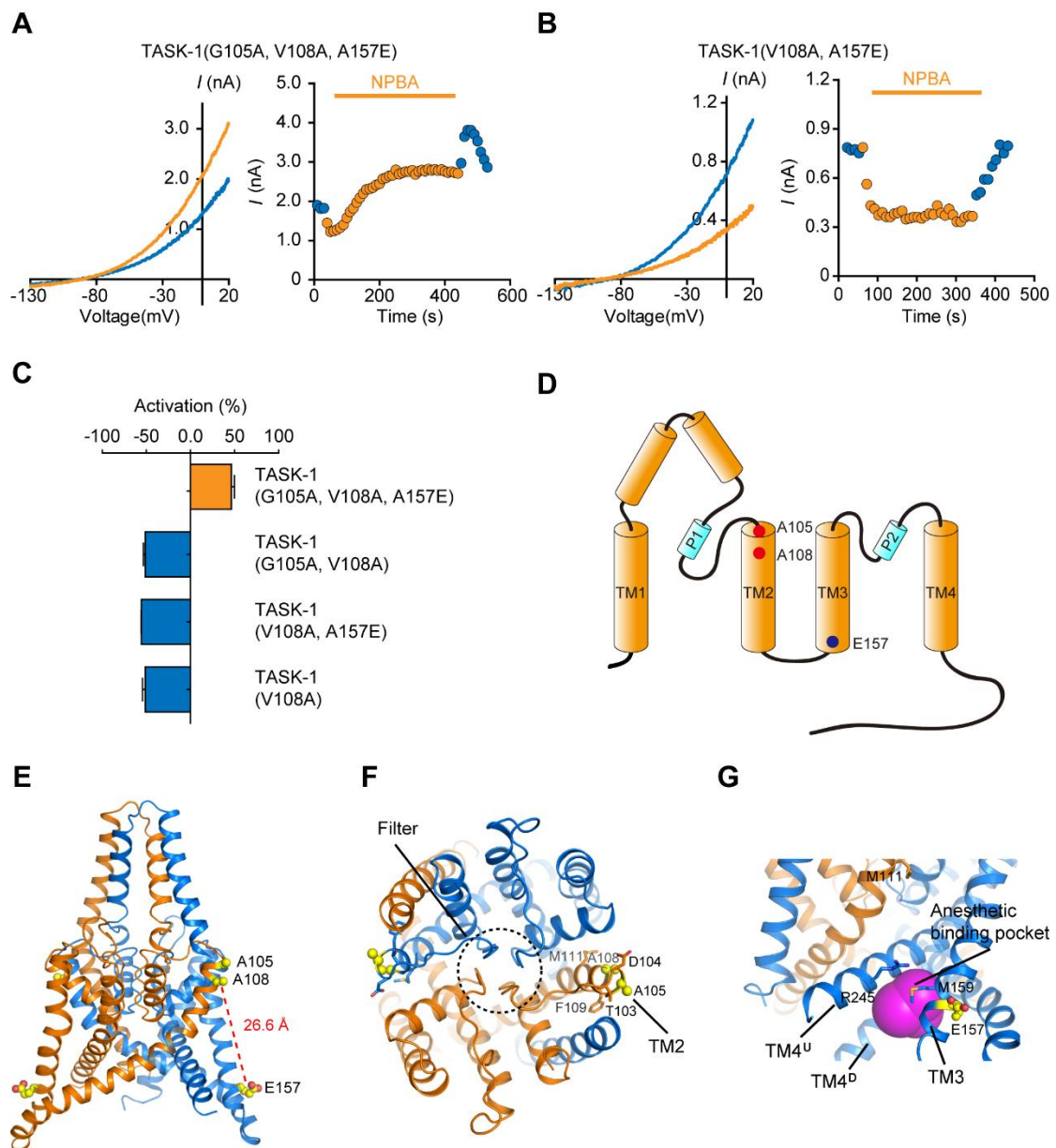
597

598

599   Figure 4

600

601

602

603   Figure 5

604

605 Figure 6

606

607

608 .